Irradiance Field Reconstruction from Partial Observability of Solar Radiation

Jonatan Ostrometzky, *Member, IEEE,* Andrey Bernstein, *Member, IEEE,* and Gil Zussman, *Senior Member, IEEE*

***Abstract*—Photovoltaic (PV) panels have become a significant source of electric power generation. These panels are considered to be one of the cleanest energy production systems available, so their spread is expected to increase in the following years, especially because recent technologies have reduced the cost of these panels. Unlike classic energy production methodologies that are connected to the high-voltage transmission power lines, many PV panels are connected directly to the lower voltage distribution networks of the electric power grid, making the management of the grid an ongoing challenge. In this paper, we address this challenge and show that the irradiance field that is required to calculate the expected power output of the PV panels can be estimated in a simplistic methodology, using partial observability of the solar radiation. We validate our proposed methodology by conducting an empirical study that uses real data of the solar radiation taken from satellites, and we show that even when the observability of the solar radiation is as low as 10% (meaning, that only 1 in 10 points of interest in a regular grid is observable), the irradiance field can be accurately estimated.**

***Index Terms*—Photovoltaic Panels, Renewable Energy, Partial Observability, Inverse Distance Weightning, Irradaince Nowcast.**

I. Introduction

There is a vast growth in photovoltaic (PV) system installation at the distribution level of the power system, particularly among residential customers, and this trend is envisioned to continue in the foreseeable future [1]. This growth creates both opportunities and challenges. Obviously, increased PV installation at the distribution level allows more flexible system operation, and decreases the dependence on traditional, fossil-fuel-based energy sources. The power output from PV sources is highly variable, and accurate estimation and prediction of this variability is essential for reliable and stable operation of the power system.

J. Ostrometzky and G. Zussman are with the EE Dept. at Columbia University, New York, NY (jio2106@columbia.edu, yonstero@gmail.com, gil@ee.columbia.edu). A. Bernstein is with the National Renewable Energy Laboratory (andrey.bernstein@nrel.gov). We would like to thank Mr. Tarek Elgindy from the National Renewable Energy Lab. His contribution with respect to accessing the solar radiation data was crucial for this research. This work was authored in part by the National Renewable Energy Laboratory (NREL), operated by Alliance for Sustainable Energy, LLC, for the U.S. Department of Energy (DOE) under Contract No. DE-AC36-08GO28308. The views expressed in the article do not necessarily represent the views of the DOE or the U.S. Government. The U.S. Government retains and the publisher, by accepting the article for publication, acknowledges that the U.S. Government retains a nonexclusive, paid-up, irrevocable, worldwide license to publish or reproduce the published form of this work, or allow others to do so, for U.S. Government purposes. This work was supported in part by the Laboratory Directed Research and Development (LDRD) Program at NREL, U.S. DOE OE as part of the DOE Grid Modernization Initiative, U.S. DOE Energy Efficiency and Renewable Energy Solar Energy Technologies Office, and DTRA grant HDTRA1-13-1-0021.

A main challenges in this context is that many PV systems are connected directly to the distribution system rather than to transmission power lines. Distribution system operators have very low observability of the system, and there is a very limited information regarding the amount of generated power from each distributed PV system in particular. The straightforward solution of requiring millions of generators to communicate with the system operator is practically infeasible for to many reasons, such as communications limitation and privacy constraints. Therefore, estimating and forecasting the PV production based on limited observation is key to enabling high penetrations of PV systems at the distribution level while maintaining reliable and stable power system operation.

Most literature on the topic focuses on extrapolating the PV-specific energy production at future times based on a sensor-based present measurements (i.e., time forecasting) [2]–[6]; whereas the spatial extrapolation of the irradiance field with resepct to PV production in low-observability conditions is mainly focused on leveraging the statistical properties of the field, via the Kriging approach (e.g., [7], [8]). These methods require training to establish the variogram of the irradiance field (i.e., the spatial correlation between the available sensors, which is both *time*- and *location*-dependant) at the specific location of interest [9], and thus are not directly applicable in cases where no past measurements with sufficiently high resolution are available.

In this paper, we focus on a "snapshot" estimation, or *nowcasting*, of PV production at different locations of the power network based on sensor measurements from limited locations in this network. We develop an interpolation scheme based on the Inverse Distance Weighting (IDW) modified Shepard's approach [10], where we consider only the input from the available sensors, and the known maximal long-term irradiance value within the interpolated area (which can be taken from the literature [11], [12]). By doing so, we show that it is possible to interpolate the full irradiance field with high accuracy, under limited sensing capabilities, without the need for high-resolution historical data.

Both the IDW [10], [13], [14] and the Kriging [13], [15], [16] methodologies are currently being used to estimate a 2-Dimensional (2-D) grid (or even a 3-Dimensional (3-D) one) from a set of available measurements in many weather-related applications (such as the estimation of rain fields from rain gauges [17], [18] or from microwave links [19], [20], after extracting the precipitation [21], [22]). These methodologies essentially treat every grid-point estimates as a single parameter, and thus they are well defined even when the sensors are sparsely located. Furthermore, under certain

sparsity conditions, a 2-D field reconstruction can be achieved using compressed sensing approaches [23].

In this work, we focus on the IDW approach, which is a deterministic interpolation approach. It is well known that the Kriging approach might achieve better results because under certain conditions [16] it is the best linear unbiased estimator [24], [25]; however, in many cases dealing with weather-related fields, it has been shown that using the IDW does not dramatically impact the resulted estimates [18], [26]. Most importantly, to implement a Kriging interpolation, one must know (or approximate) certain statistical properties of the field of interest [27], which is generally not known. By implementing an IDW approach rather than either a Kriging or a compressed sensing approaches, our developed tool could be implemented directly on any region of interest, without the need of any prior knowledge regarding the field's statistical or sparsity properties, and provide with deterministic and consistent results.

The rest of this paper is organized as follows: In Section II, we present our methodology and develop the field estimation tool. In Section III, we demonstrate and validate our tool using a real-world yearlong experiment. Last, in Section IV, we conclude the paper and discuss future research opportunities.

II. Methodology

Define a 2-D field of irradiance representing the Global Horizontal Irradiance (GHI) values (in W/m^2), as $I_r(x, y, t)$. Our goal is to reconstruct the irradiance field in a given area of interest and at a given time. In other words, $I_r(x, y, t_j)$ is to be estimated $\forall\{0 \leq x \leq A, 0 \leq y \leq B\}$, for a given time index, t_j, where A and B are the boundaries of the respected area of interest.

Next, we can define:

$$\theta_i^j \equiv I_r(x_i, y_i, t_j) \tag{1}$$

where θ_i^j is the value of the irradiance (in W/m^2) at a given location, $\{x_i, y_i\}$, at time index, t_j.

A. Problem Statement

To reconstruct the irradiance field for time index t_j, we require estimating a set of θ_i^j, where $i \in \{1, 2, \cdots, N\}$, so that the set of $\{x_i, y_i\}$ represents a regular 2-D grid spanning $\{0 \leq x \leq A, 0 \leq y \leq B\}$. Note that the resolution of the reconstructed field is determined by the value of N. Once the estimates $\hat{\theta}_i^j$ are found $\forall\{i, j\}$, the full continuous irradiance field, $I_r(x, y, t)$, can be directly reconstructed using standard methodologies such as the nearest-neighbor [28], the cubic [29], and the spline [30] methods.

We assume that we have access to a set of measurements (i.e., samples) of the actual GHI values within the field. The GHI measurements can be taken either directly (via weather stations or dedicated equipment), or by using the PV systems, given that the PV installation angle is known and the current (I) and the voltage (V) status (also known as the IV curve) of the PV panels are being regularly monitored and reported [31].

As stated in Section I, we aim to reconstruct the irradiance field under conditions of low or partial observability (e.g., only a small number of GHI sensors are available, or only a small part of the PV systems connected to the distribution grid in a given area are being monitored for the IV status by the utility company). Thus, we assume that within the given area of interest at time index j, the number of estimates, $\hat{\theta}_i^j \; ; \; i \in \{1, 2, \cdots, N\}$, is to be estimated based on a set of GHI measurements, $r_k^j \; ; \; k \in \{1, 2, \cdots, K\}$, where $K < N$, or, at some scenarios, $K << N$.

Note, that although the arrangement of the grid of θ_i^j follows a regular grid, and its density is dictated by N (and translates into the resolution of the interpolated irradiance field), the locations of r_k^j are arbitrary. **Fig. 1** illustrates a rectangular area divided by a regular grid of 551 points (i.e., $N = 551$) for a given time index. The use of $N = 551$ in this specific grid formation is chosen in order to correspond with the real-world experimental setup that will be presented in the sequel.

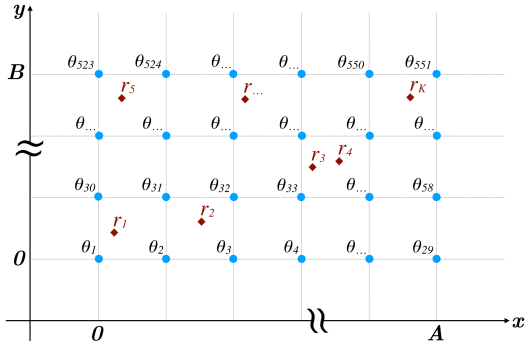

Fig. 1. Illustration of an area of interest, $I_r(x, y, t_j) \in \{0 \leq x \leq A, 0 \leq y \leq B\}$, and $\theta_i^j \; ; \; i \in \{1, 2, \cdots, 551\}$ estimates. In addition, the available GHI sensors (each produces a single GHI sample at that given time index) are marked by r_i. For simplicity, the time index superscript is dropped.

B. Irradiance Field Interpolation

Our goal is to compute each estimate $\hat{\theta}_i^j$ within a given area and at the relevant time indexes. For simplicity, from now on, we focus on estimating the irradiance field for a single time index, t_j. Thus, in the sequel, we drop the superscript j.

Let $\vec{\theta} \equiv [\theta_1, \theta_2, \cdots, \theta_N]^T$ and $\vec{r} \equiv [r_1, r_2, \cdots, r_K]^T$ denote the parameter and measurement vectors, respectively. Observe that as $\vec{\theta} \in \mathcal{R}^N$, $\vec{r} \in \mathcal{R}^K$, with $K < N$, implementing a parameter estimation processes, either deterministic such as the weighted least squares or statistic such as the Maximum Likelihood estimation, are infeasible. On the other hand, the IDW and Kriging methodologies treat every grid-point estimate as a single parameter, and thus they are well defined even when the sensors are sparsely located. As advocated in Section I, this paper focuses on the application of the IDW method to the problem at hand, which is detailed next.

C. Modified Shepard's-Like Approach

To estimate any of the grid points, θ_i, we use the Modified Shepard's interpolation [10]. The Modified Shepard's interpolation closely resembles the standard IDW [13], but adds

a conditional distance rule. In particular, for each estimated grid point, only the sensors (i.e., the available measurements) located within a given Radius Of Influence (ROI) around the relevant grid point are taken into account.

One of the properties of the standard modified Shepard's approach is that the grid points are always smaller or equal to the maximum sampled value. This fact is desired in cases such as rain-field interpolation from rain-gauges data because an interpolated rain-field grid point is nullified if no rain gauge is located inside its ROI. In our scenario, using this approach without modification will result in a negative bias that will be introduced into the estimation. We therefore use *the disturbance-free GHI value* for interpolated grid points with no sensor is located inside its ROI. This disturbance-free value is the maximal possible GHI value in the area of interest. In a real-world application, this maximum value can be taken from the literature (e.g., [11], [12]), or by using very low-resolution measurements that are widely available. Thus, the estimation of $\hat{\theta}_i$ can be formalized using the weighting function $w(\cdot)$:

$$\hat{\theta}_i = \begin{cases} \frac{\sum_{k=1}^{K} r_k \cdot w(d_{ik},p,R)}{\sum_{k=1}^{K} w(d_{ik},p,R)} & ;\sum_{k=1}^{K} w(d_{ik},p,R) > 0 \\ I_r^{max} & ;\sum_{k=1}^{K} w(d_{ik},p,R) = 0 \end{cases} \quad (2)$$

$$w(d_{ik},p,R) = \begin{cases} \frac{\left(1-\frac{\sqrt{d_{ik}}}{R}\right)^p}{\left(\frac{\sqrt{d_{ik}}}{R}\right)^p} & ;d_{ik} \le R^2 \\ 0 & ;d_{ik} > R^2 \end{cases} \quad (3)$$

$$d_{ik} = (x_i - x_k)^2 + (y_i - y_k)^2 \quad (4)$$

where R is the specific ROI, $\{x_i, y_i\}$ and $\{x_k, y_k\}$ are the coordinates of θ_i and r_k respectively, and p is a coefficient that dictates the decay rate of $w(\cdot)$. In weather-related applications, p is usually set to $p = 2$ [17], [32]. I_r^{max} is the maximum (or approximated maximum) GHI value (in W/m^2) within the respected area of interest (at the relevant time index):

$$I_r^{max} = \max_{\substack{0\le x\le A \\ 0\le y\le B}} \{I_r(x,y,t_j)\} \quad (5)$$

D. ROI Selection Consideration

The ROI, R, is a design parameter that dictates the geographical radius around a sensor in which the sensor's measurements will affect the estimated GHI field. Estimating $\hat{\theta}_i$ by using only measurements taken from the area inside a given ROI makes sense because any large-scale disturbance to the irradiance (such as a cloud, foliage, shade, etc.) is almost certainly confined to a specific location, and will not affect the irradiance field outside of a given radius. Thus, on one hand, it is important to select a sufficiently large ROI so that the sensor-measured information will be fully incorporated into the interpolation, especially when the sensors are sparse. On the other hand, the information provided by a specific sensor is location based, and thus, it is physically limited (i.e., a disturbance in the GHI field (caused by, e.g., clouds) is location limited). To insure these two demands when selecting a specific ROI, we suggest to considering *the averaged cloud size*, as clouds are the main cause of disturbance in the GHI field. In [33], it was suggested that the standard Cumulus-cloud size follows the Log-Normal distribution, with a mean size of a few kilometers and a standard deviation of a few kilometers. In [34], the authors present a detailed Large-Eddy simulation and suggest that the horizontal domain size of a general cloud is roughly 3.2 km to 12.8 km.

Based on these conjectures, in the sequel, we use $R = 20$ and $R = 28$ km, which should be sufficiently large to cover the majority of the rain-causing Cumulus clouds. Indeed, the ROI value may be optimized for a given location based on the position and the sparsity of the available sensors, as well as the location-specific climate, which remains a subject of future research. Nonetheless, based on the the experimental validation presented in the sequel, the resulting GHI field estimation did not change in a significant manner based on the selected ROI, which suggests that the presented approach is reasonably robust with respect to the choice of the ROI.

III. Experimental Validation

To validate our approach, we designed a real-world experiment based on actual solar data. The data used were collected via the National Renewable Energy Laboratory initiative (NSRDB). The data were collected via half-hourly radiance images from the GOES weather satellites. These, in combination with snow coverage, temperature, and pressure profiles - were used to produce the GHI values in 30-minute intervals. The measurements are recorded as the averaged GHI within cells, with a spacial resolution of 0.038 degrees latitude and 0.038 degrees longitude per cell [12]. From the NSRDB database, we collected and analyzed the GHI measurements from an area of interest, located between $40.57N$ and $41.29N$ degrees latitude, and $73.50W$ and $74.62W$ degrees longitude. This area includes 19*29 cells (with a total area[1] approximated to be 76*116 km^2) covering the city of New York and its surroundings. A map of the selected area with the division into the specific cells is depicted in **Fig. 2**.

A. Experiment Description

Each of the $4 * 4$ km^2 cells that comprise the selected area (depicted in **Fig. 2**) is treated as a single estimation point θ_i. Thus, in this scenario[2], $N = 19 * 29 = 551$.

We performed the estimation process for each of the 551 grid points (i.e., the set of $\hat{\theta}_i$ of Eq. (2), where $i \in \{1, 2, \cdots, 551\}$) as follows:

1) A set of $K = round(0.9 * 551)$ sensors, r_k ; $k = \{1, 2, \cdots, K\}$, were chosen and located randomly within the selected area. The ROI was chosen to be either $R = 20$ km or $R = 28$ km.

[1]Please note that the transformation between a fixed value of 0.038 degrees latitude and/or longitude into the distance and/or surface area measured in kilometers depends on the specific location (due to the Earth's curvature). Nonetheless, in the location of interest, the differences between individual tiles are negligible, and, for simplicity, we approximated each cell to have the surface area of 4*4 km^2.

[2]Using the formulation of Eq. (5) results in: $0 \le x - 73.50 \le A$, and $0 \le y - 40.57 \le B$, where $A = 74.62 - 73.50$ and $B = 41.29 - 40.57$.

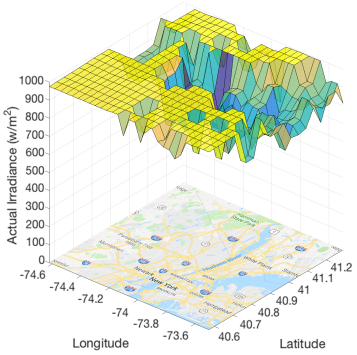

Fig. 2. Map of the selected area, divided into 19*29 cells of $\approx 4 * 4$ km^2 (captured via Google Maps), and the actual irradiance field as calculated based on the NSRDB on 12:00, June 21, 2014.

2) The actual GHI value of each of the sensors r_k were taken from the NSRDB data set, for January 1, 2014, at 12:00 EST.
3) The value of I_r^{max} was taken from the recorded by the NSRDB data set of the entire selected area on January 1^{st}.
4) Steps 1 - 3 were repeated 100 times, each time with a different set of random r_k (causing a different placement of the sensors).
5) Steps 1 - 4 were repeated 365 times, for every day within the year 2014, at 12:00:00 local time.
6) Steps 1 - 5 were repeated for different values of $K = round(s * 551)$, where $s \in \{0.9, 0.8, 0.7.0.6, 0.5, 0.4, 0.3, 0.2, 0.1, 0.05\}$ represents the percentage of grid cells with an observable GHI sensor.

B. Results

Overall, the value of each grid cell was estimated via Eq. (2) $36,500$ times for each value of s. Using all of the 551 grid cells, a total of $20,111,500$ cells were estimated per value of s, for R =20 km and R =28 km. To analyze the resulted interpolation, the Root Mean Squared Error (RMSE) between all of the $20,111,500$ estimates and the actual cells GHI values (taken from the available NSRDB data set, and calculated after the grid cell used as sensors input data are excluded) was calculated. The resultant RMSE as a function of the number of available GHI sensors, for both cases where R =20 km and R =28 km, are depicted in **Fig. 3.** In addition, the same experiment (as described in Section III-A) was repeated daily at 08:00:00 and 16:00:00 local times, and the respective RMSE results are also depicted in **Fig. 3**. Furthermore, examples of the full scatter plots of the entire $20,111,500$ estimated grid cells vs. the actual GHI values as reported by the NSRDB, for R =20 km with $s = 0.8$ and $s = 0.1$, are depicted in **Fig. 4**, and **Fig. 5**, respectively.

IV. Discussion and Conclusion

From the results presented in Section III-B, it can be concluded that the 2-D irradiance field can be interpolated in relatively high accuracy in most cases, even in cases where as little as only 10% (i.e., $s = 0.1$) of the grid cells is observable.

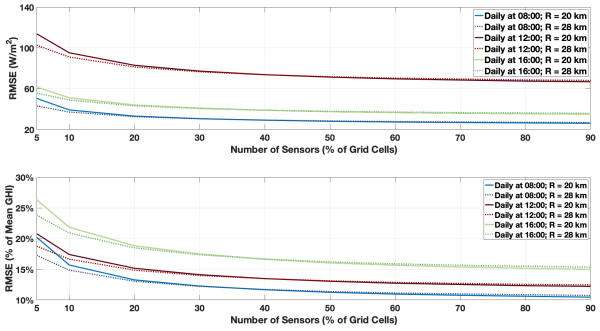

Fig. 3. The RMSE between the estimated grid cells and the actual GHI values (as reported by the NSRDB, excluding the cells used as the the sensors input data), as a function of the number of observable GHI sensors, for 08:00:00, 12:00:00, and 16:00:00 local times, throughout the year 2014. The actual RMSE is presented in the top panel, and the RMSE in the sense of percentage of the total averaged measured GHI value (calculated for each time) is presented in the bottom panel.

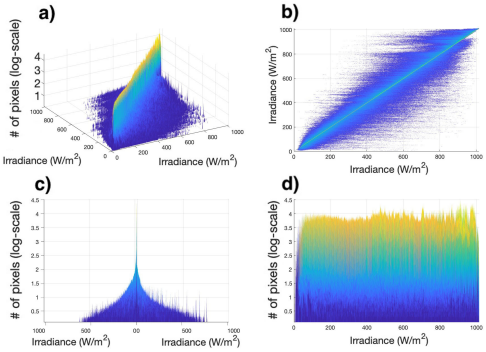

Fig. 4. Scatter plot (in log-scale) of the estimated grid cells based on GHI sensors located at 80% of the cells ($s = 0.8$), on January 1 to December 31, 2014, at 12:00:00, vs. the actual GHI NSRDB-reported values. Shown are 3-D (a), top (b), front (c), and side (d) views.

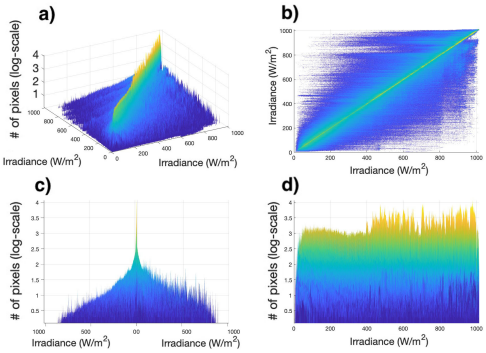

Fig. 5. Scatter plot (in log-scale) of the estimated grid cells based on GHI sensors located at 10% of the cells ($s = 0.1$). See **Fig. 4** for details.

Specifically, **Fig. 3** shows that the relative RMSE between an estimated grid cell and the actual GHI value for a case where $s = 0.1$ is less than than 22%, regardless of the time of day (and thus, regardless of the angle of the sun or the maximum GHI within the area).

A few further challenges require future research. First, in this experiment, the ROI was taken to be R =20 km and R =28 km. Although we did not detect any meaningful

change in the resulting RMSE when different ROI values were chosen, **Fig. 3** shows that the larger selected ROI (R =28 km) produced better results for the cases where the number of sensors is very low (i.e., $\leq 20\%$, whereas the smaller ROI tested (R=20 km) produced slightly better results for when the observability is higher. As mentioned in Section II-D, we believe that the ROI coefficient selection could be optimized based on the sparsity of the available sensors, especially if the local climate (such as the size of the average clouds) is known, and, can potentially improve the accuracy of the irradiance-field estimation. Second, as shown in **Fig. 4** and **Fig. 5**, there is a small bias in the estimation of the grid cells towards the higher GHI values. We believe this bias is caused by our modification of the estimation process presented in Eq. (2), which results in the estimate $\hat{\theta}_i$ being equal to the maximum GHI value measured (or assumed), I_r^{max}, in cases where the closest GHI sensors, r_k, are located (relative to the location of θ_i) outside the ROI. Future enhancement such as iterative estimation algorithms (which, might also incorporate the irradiance temporal changes) might be able to compensate for this bias. Nonetheless, in all cases, the spatial correlation coefficients between the estimated grids and the actual NSRDB ground-trugh grids, for all the values of s and R tested, were higher than 0.9. Furthermore, we performed a multi-variable cubic interpolation (based on the approach described in [6]) on the same experimental setup (of Section III), and compared the resulted interpolated irradiance field with our presented approach: Our approach out-performed the multi-variable interpolation (with respect to the RMSE and the correlation coefficients values) for all cases (R =20 km), and for all cases when $s \geq 0.1$ (R =28 km). To conclude, we believe that the feasibility study presented in this paper is promising and shows that the irradiance field can be interpolated accurately in a simplistic formulation, under limited observability conditions.

REFERENCES

[1] T. Mai, R. Wiser, G. Barbose, L. Bird, J. Heeter, D. Keyser, V. Krishnan, J. Macknick, and D. Millstein, "A prospective analysis of the costs, benefits, and impacts of us renewable portfolio standards," tech. rep., National Renewable Energy Lab.(NREL), Golden, CO, USA, 2016.

[2] P. Bacher, H. Madsen, and H. A. Nielsen, "Online short-term solar power forecasting," *Solar Energy*, vol. 83, no. 10, pp. 1772–1783, 2009.

[3] R. Perez, K. Moore, S. Wilcox, D. Renné, and A. Zelenka, "Forecasting solar radiation–preliminary evaluation of an approach based upon the national forecast database," *Solar Energy*, vol. 81, no. 6, pp. 809–812, 2007.

[4] J. Huang, M. Korolkiewicz, M. Agrawal, and J. Boland, "Forecasting solar radiation on an hourly time scale using a coupled autoregressive and dynamical system (cards) model," *Solar Energy*, vol. 87, pp. 136–149, 2013.

[5] A. Mellit and A. M. Pavan, "A 24-h forecast of solar irradiance using artificial neural network: Application for performance prediction of a grid-connected pv plant at trieste, italy," *Solar Energy*, vol. 84, no. 5, pp. 807–821, 2010.

[6] A. T. Lorenzo, W. F. Holmgren, and A. D. Cronin, "Irradiance forecasts based on an irradiance monitoring network, cloud motion, and spatial averaging," *Solar Energy*, vol. 122, pp. 1158–1169, 2015.

[7] A. Bodas-Salcedo, E. López-Baeza, F. Martínez, J. Mateu, and F. Montes, "Spatiotemporal modeling and prediction of solar radiation," *Journal of Geophysical Research: Atmospheres*, vol. 108, no. D24, 2003.

[8] M. Jamaly and J. Kleissl, "Spatiotemporal interpolation and forecast of irradiance data using kriging," *Solar Energy*, vol. 158, pp. 407–423, 2017.

[9] C. A. Gueymard and S. M. Wilcox, "Assessment of spatial and temporal variability in the us solar resource from radiometric measurements and predictions from models using ground-based or satellite data," *Solar Energy*, vol. 85, no. 5, pp. 1068–1084, 2011.

[10] D. Shepard, "A two-dimensional interpolation function for irregularly-spaced data," in *Proceedings of the 1968 23rd ACM national conference*, pp. 517–524, ACM, 1968.

[11] J. Suh and Y. Choi, "Methods for converting monthly total irradiance data into hourly data to estimate electric power production from photovoltaic systems: A comparative study," *Sustainability*, vol. 9, no. 7, p. 1234, 2017.

[12] "NREL Irradiance Database Viewer; NSRDB," *https://maps.nrel.gov/nsrdb-viewer/*.

[13] R. Franke, "Scattered data interpolation: tests of some methods," *Mathematics of computation*, vol. 38, no. 157, pp. 181–200, 1982.

[14] C. Daly, W. P. Gibson, G. H. Taylor, G. L. Johnson, and P. Pasteris, "A knowledge-based approach to the statistical mapping of climate," *Climate research*, vol. 22, no. 2, pp. 99–113, 2002.

[15] M. L. Stein, *Interpolation of spatial data: some theory for kriging*. Springer Science & Business Media, 2012.

[16] N. Cressie, "The origins of kriging," *Mathematical geology*, vol. 22, no. 3, pp. 239–252, 1990.

[17] F.-W. Chen and C.-W. Liu, "Estimation of the spatial rainfall distribution using inverse distance weighting (idw) in the middle of taiwan," *Paddy and Water Environment*, vol. 10, no. 3, pp. 209–222, 2012.

[18] K. Dirks, J. Hay, C. Stow, and D. Harris, "High-resolution studies of rainfall on norfolk island: Part ii: Interpolation of rainfall data," *Journal of Hydrology*, vol. 208, no. 3-4, pp. 187–193, 1998.

[19] A. Overeem, H. Leijnse, and R. Uijlenhoet, "Country-wide rainfall maps from cellular communication networks," *Proceedings of the National Academy of Sciences*, vol. 110.8, pp. 2741–2745, 2013.

[20] H. Messer and O. Sendik, "A new approach to precipitation monitoring," *IEEE Signal Processing Magazine*, pp. 110–122, 2015.

[21] J. Ostrometzky, D. Cherkassky, and H. Messer, "Accumulated precipitation estimation using measurements from multiple microwave links," *Adv. Meteorology*, vol. Special Issue (PRES), 2015.

[22] J. Ostrometzky and H. Messer, "Dynamic determination of the baseline level in microwave links for rain monitoring from minimum attenuation values," *IEEE Journal of Selected Topics in Applied Earth Observations and Remote Sensing*, vol. 11, no. 1, pp. 24–33, 2018.

[23] L. Gazit and H. Messer, "Sufficient conditions for reconstructing 2-d rainfall maps," *IEEE Trans. on Geoscience and Remote Sensing*, no. 56/11, pp. 6334–6343, 2018.

[24] J. Guo-Dong, L. Yan-cong, and N. Wen-Jie, "Comparison between inverse distance weighting method and kriging," *Journal of Changchun University of Technology*, vol. 3, 2003.

[25] D. Zimmerman, C. Pavlik, A. Ruggles, and M. P. Armstrong, "An experimental comparison of ordinary and universal kriging and inverse distance weighting," *Mathematical Geology*, vol. 31, no. 4, pp. 375–390, 1999.

[26] B. I. Harman, H. Koseoglu, and C. O. Yigit, "Performance evaluation of idw, kriging and multiquadric interpolation methods in producing noise mapping: A case study at the city of isparta, turkey," *Applied Acoustics*, vol. 112, pp. 147–157, 2016.

[27] T. Inoue, T. Sasaki, and T. Washio, "Spatio-temporal kriging of solar radiation incorporating direction and speed of cloud movement," in *The 26th Annual Conference of the Japanese Society for Artificial Intelligence*, 2012.

[28] T. Cover and P. Hart, "Nearest neighbor pattern classification," *IEEE Transactions on Information Theory*, vol. 13, no. 1, pp. 21–27, 1967.

[29] J. A. Parker, R. V. Kenyon, and D. E. Troxel, "Comparison of interpolating methods for image resampling," *IEEE Transactions on medical imaging*, vol. 2, no. 1, pp. 31–39, 1983.

[30] C. de Boor, "A practical guide to splines," *Applied Mathematical Sciences, New York: Springer, 1978*, 1978.

[31] T. Salmi, M. Bouzguenda, A. Gastli, and A. Masmoudi, "Matlab/simulink based modeling of photovoltaic cell," *Int. Journal of Renewable Energy Research (IJRER)*, vol. 2, no. 2, pp. 213–218, 2012.

[32] B. Ahrens, "Distance in spatial interpolation of daily rain gauge data," *Hydrology and Earth System Sciences Discussions*, vol. 2, no. 5, pp. 1893–1922, 2005.

[33] R. E. López, "The lognormal distribution and cumulus cloud populations," *Monthly Weather Review*, vol. 105, no. 7, pp. 865–872, 1977.

[34] R. Neggers, H. Jonker, and A. Siebesma, "Size statistics of cumulus cloud populations in large-eddy simulations," *Journal of the atmospheric sciences*, vol. 60, no. 8, pp. 1060–1074, 2003.